Optics Communications 281 (2008) 3985–3989

Contents lists available at ScienceDirect

Optics Communications

journal homepage: www.elsevier.com/locate/optcom

Using a micro-molding process to fabricate polymeric wavelength filters

Wei-Ching Chuang [a], An-Chen Lee [b,c], Chi-Ting Ho [b,*]

[a] Department of Electro-Optics Engineering, National Formosa University, Huwei 632, Yulin, Taiwan
[b] Department of Mechanical Design Engineering, National Formosa University, 64 Wen Hua Road, Huwei 632, Yulin, Taiwan
[c] Department of Mechanical Engineering, National Chiao-Tung University, Hsinchu 300, Taiwan

ARTICLE INFO

Article history:
Received 7 December 2007
Received in revised form 30 March 2008
Accepted 3 April 2008

Keywords:
Holographic interferometry
Optical fabrication
Diffraction gratings
Mold
Polymeric wavelength filters

ABSTRACT

A procedure for fabricating a high aspect ratio periodic structure on a UV polymer at submicron order using holographic interferometry and molding processes is described. First, holographic interferometry using a He–Cd (325 nm) laser was used to create the master of the periodic line structure on an i-line sub-micron positive photoresist film. A 20 nm nickel thin film was then sputtered on the photoresist. The final line pattern on a UV polymer was obtained from casting against the master mold. Finally, a SU8 polymer was spun on the polymer grating to form a planar waveguide or a channel waveguide. The measurement results show that the waveguide length could be reduced for the waveguide having gratings with a high aspect ratio.

© 2008 Elsevier B.V. All rights reserved.

1. Introduction

Gratings are used in integrated optics for several purpose, including wavelength filtering, sensing, optical measuring technique, spectral narrowing of laser output, optical power coupling in waveguide systems, etc. [1–6]. In particular, surface grating with high diffraction efficient can be utilized in many applications, such as holographic image storage, liquid crystal anchoring, optical filters, or resonant couplers [7]. In surface grating applications, the grating depths significantly affect the performance of optical devices [7,8]. If grating-assisted waveguides are used in optical filter applications, shallow grating, which will result in small coupling coefficients, will lead to an unfeasibly narrow transmission bandwidth and will therefore require a long coupling length to attain a specific transmission [9]. Furthermore, when optical light sources with a short wavelength are used in optical components, the higher-order peaks of propagation modes cannot be eliminated from the filter; this will result in low efficiency of the first-order peak of propagation modes if the aspect ratio between the depth and the period of gratings is low [9]. A deep waveguide Bragg grating is of interest in practical application such as semiconductor waveguides [10] or input–output coupler in integrated-optics [11,12]. Recently, Zhu et al. demonstrated polymeric multi-channel band pass filters [13] and optical add-drop multiplexers [14] with corrugated sidewall Bragg grating using deep grating. Their results showed that the grating length can be shortened to around 500 μm.

The conventional method for fabricating grating involves patterning and etching. Typical techniques used for patterning gratings on polymer waveguides include soft lithography [15], proximate-contact lithography on a silicon–nitride grating [16], and nanoimprint technique [17]. Kocabas and Aydinli reported the fabrication of a grating on OG 146 polymer using soft lithography, e-beam direct writing, and stamp transfer techniques [15]. Then, a BCB polymeric ridge waveguide was fabricated on the grating using reaction ion etching technique. The grating fabrication process is similar to our previous work except for the e-beam writing technique [18]. In proximate-contact lithography and nanoimprint technique, the gratings were fabricated on silicon-nitride or quartz stamps by the RIE technique. The aspect ratio of the gratings can be controlled by varying the etching rate of the RIE.

Kim et al. fabricated Bragg grating using the nanoimprint technique to successfully transfer the grating pattern onto a polymer layer [19]. The nanoimprint process is cost effective and simple method for fabricating a stamp. However, it has certain drawbacks, as explicitly mentioned in Ref.15. These drawbacks may restrict the use of this method in fabricating a Bragg grating filter. In these techniques, the RIE process transfers a grating pattern from the top polymer layer to the core underneath and it increases the difficulty of obtaining accurate and smooth waveguide gratings [14]. For soft lithography, Schmid and Michel used a rigid PDMS, "h-PDMS", to fabricated periodic structure with feature size below 100 nm and aspect ratio (as their definition depth/width of pattern) 1.25 [20]. Lee et al. also demonstrated high aspect ratio periodic structures using h-PDMS and show good stamp transfer fidelity when compared with general PDMS. In their experiment, the aspect ratio

* Corresponding author. Tel.: +886 56315195 fax: +886 56338302.
E-mail address: hoct@ms25.hinet.net (C.-T. Ho).

0030-4018/$ - see front matter © 2008 Elsevier B.V. All rights reserved.
doi:10.1016/j.optcom.2008.04.019

reached 4.2 with period below 1500 nm [21]. However, the main drawbacks of h-PDMS are the brittle nature of h-PDMS and the thermal curing requirements of such material. Because the relatively low toughness of the h-PDMS made relief features with these geometries susceptible to fracture, elements of h-PDMS tended to fail due to fracture of the relief features during fabrication of the elements or during their use, particularly in molding applications [22]. In this paper, grating patterns on the photoresist are prepared by the holographic interferometric technique. This technique offers important advantages compared to other techniques in that it can easily control the period and depth of gratings, and it is more naturally suited to the production of high-resolution gratings than other techniques, yielding good uniformity of the grating period with greater ease. In addition, the theoretical limit of the frequency of the interference pattern produced by two intersecting beams is half the wavelength of the incident beam. Thus, the grating period is limited only by the wavelength of the light source.

The materials used as well as the fabrication processes are important factors in manufacturing optical elements for different applications. Sol–gel hybrid (SGH) materials can be easily used for the fabrication of grating diffraction by the holographic interferometric technique; however such material cannot be used for the fabrication of grating pattern with high aspect ratios, and since they are brittle material, they are hard to be used as any applied applications [23]. In our previous paper [18], our polymer diffraction gratings were fabricated using the holographic interferometric technique with a photoresist (Ultra 123) to obtain a grating pattern with a high aspect ratio. Then, the patterned resist was used as a master mold to transfer the pattern onto a polydimethylsiloxane (PDMS, rubber) thin film, which was cast against the patterned resist. However, it was observed that when the depth of the grating was larger than 350 nm, which is accompanied by a grating period smaller than 500 nm, some of the gratings appeared to affix to the bottom and to each other after release from the photoresist mold. These structures appeared as though the grating period had been broadened. This sticking effect is also observed, when the aspect ratio between the depth and the period is greater than 0.7. This sticking effect increased with the aspect ratio because the fins are less rigid. Therefore, in this paper we present a technique wherein the holographic interferometric and micromolding process to create a grating structure with a high aspect ratio on a polymer waveguide.

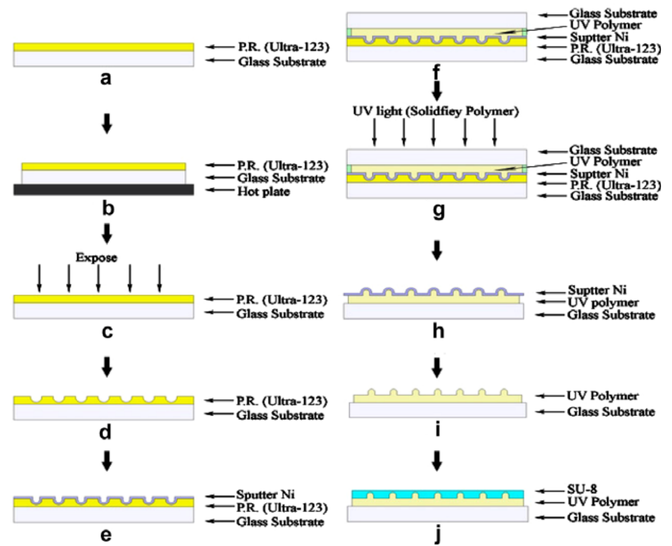

Fig. 1. Schematic illustration of the polymeric waveguide filter fabrication.

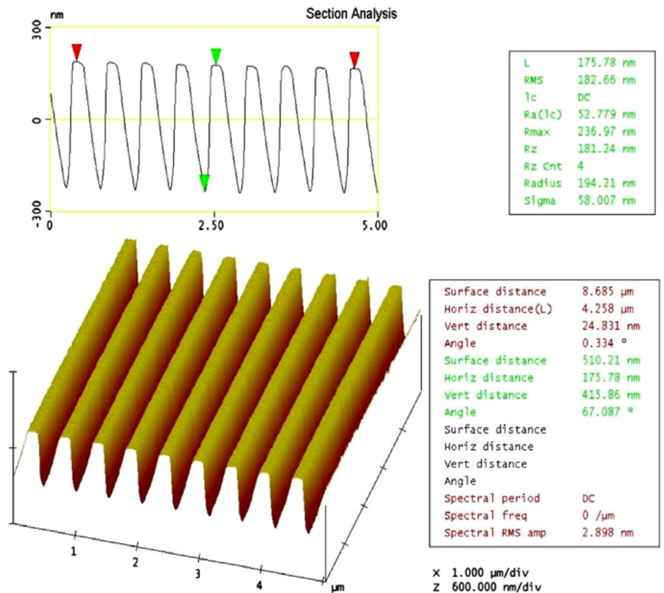

Fig. 2. The AFM picture and measurement result for the grating on photoresist 508 nm grating period.

2. Methodology

The technique of forming grating patterns on the UV polymer involves three processing steps. First, a grating pattern is holographically exposed using a two-beam interference pattern on a positive photoresist film. A 20-nm-thick nickel thin film is then sputtered onto the positive photoresist mold. This mold can be subsequently used to transfer the final gratings pattern onto a UV cure epoxy polymer. The following sections describe the process involved in grating fabrication.

The master grating patterns on a positive photoresist (Ultra123, Microchem. Corp. MA) were holographically exposed using a two-beam interferometer technique (Fig. 1a–d). The details of this process have been described in previous reports [18]. Based on our results, we found that the grating period and the corresponding depth of the grating pattern can be accurately controlled down to an error rate of less than 1%. We also found that a high aspect ratio of almost 1:1 between the depth and the period of the grating structure could be obtained using this process. The profiles of the grating were measured by using an atomic force microscope (AFM). Fig. 2 showed the AFM result of the photoresist with a grating period and grating depth of 530 nm and 416 nm. The surface roughness of the grating is around 1 nm.

Since the adhesion between the photoresist (Ultra 123) and the other polymers is strong, the polymers cannot be easily separated from Ultra 123. On the other hand, the Ni metal is easily to be etched away from any polymers by the $FeCl_3$ etching solution. A nickel thin film was then sputtered onto the positive photoresist mold by an RF sputtering system for 1 min (Fig. 1e). The power source is 50 W, and the pressure is restricted to less than 5×10^{-3} Torr. The thickness of nickel is approximately 20 nm. The profiles of the metal molds were measured using an atomic force microscope (AFM). A table comparing the grating geometry on the metal and photoresist molds shows that the overall dimension was reduced when patterns were transferred from the photoresist to the metal (Table 1). These results indicated an average reduction of 0.41% or 2.7 nm in the periods. On the other hand, the average reduction in depths was reduced by as much as 13.7% and 14–36 nm.

The final pattern was transferred onto three types of cure epoxy substrate having different shrinkage ratio using an injected

Table 1
Results of gratings from the SEM and AFM measurement on photoresist (PR), Ni, and UV polymers

Master grating mold (Ultra123)		Master mold with Ni		Polymer grating (UV)		Ultra123 to polymer error	
Period (nm)	Depth (nm)	Period (nm)	Depth (nm)	Period (nm)	Depth (nm)	Period (nm)	Depth (nm)
508	192	506	173	(1)505	172	$3_{(0.6\%)}$	$20_{(10.4\%)}$
508	274	506	253	(1)501	253	$7_{(1.4\%)}$	$21_{(7.7\%)}$
508	393	503	371	(1)494	366	$14_{(2.8\%)}$	$27_{(6.8\%)}$
508	263	506	227	(2)501	208	$7_{(1.4\%)}$	$54_{(21\%)}$
508	363	505	347	(2)501	301	$7_{(1.4\%)}$	$62_{(17\%)}$
505	372	503	348	(2)491	296	$14_{(2.8\%)}$	$76_{(20\%)}$
514	162	511	146	(3)514	125	$10_{(1.9\%)}$	$37_{(23\%)}$
514	276	510	255	(3)514	206	$11_{(2.1\%)}$	$70_{(25.3\%)}$
514	377	512	350	(3)513	283	$11_{(2.1\%)}$	$94_{(25.1\%)}$

(1) OG146 with a shrinkage ratio 0%. (2) AT9575 with a shrinkage ratio 4%. (3) AT8105 with a shrinkage ratio 6%.

molding process from the positive photoresist mold that was sputtered on nickel (Fig. 1f–i). The solidified reaction of polymers often results in volume contraction because water or other solvent byproduct is released out after reaction. However, in the case of the OG 146 polymer, almost no water or solvent byproduct is released out after reaction [24,25]. The fabrication procedure is described as follows. A spacer with thickness 400 μm was placed between the mold and a thin Pyrex glass slide. The mold was supported by another Pyrex glass slide to create a support for the positive photoresist mold. After injecting the precure UV polymers (OG146, Epoxy Technology Inc., AT9575, AT8105, NTT Inc.) into the opening between the mold and the glass slide by using a fine tip syringe, the liquid solution automatically spread and filled up the space between the mold and slide. A UV curing lamp with a wavelength range of 300–400 nm was used to crosslink the polymer at an intensity of 100 mW/cm^2 for 1–2 min. After the polymer was fully cured, the sample was immersed in an acetone solution to remove the positive photoresist. The sample was then immersed in a $FeCl_3$ solution ($FeCl_3$:H_2O = 1:1; solution' temperature was maintained at 25 °C) to remove nickel, and the final gratings are formed on the UV polymer.

The AFM and SEM measurements of the gratings on a UV polymer are listed in Table 1. The AFM and SEM micrographs of the gratings on a UV polymer show OG146 polymer gratings with a 532 nm period and 418 nm depth, indicating that a periodical structure with a high aspect ratio can be obtained by using the above-mentioned fabrication process (Fig. 3). We can conclude that when the shrinkage ratio of the polymer is large, the reduction in the grating dimension appears to be higher (Table 1). For example, when the shrinkage ratio of the polymer is 6%, the grating period and depth can be reduced by as much as 2.2% and 25.3% respectively, when patterns are transferred from the photoresist to UV polymer. Overall, for OG146 polymer, the depth reduced by an average of around 8.2% from the original photoresist mold, and the period was transferred much better when an average reduction of 1.6% occurred when pattern transforming the photoresist to UV polymer. For the OG146 polymer grating, which has a modulation depth of 418 nm, a transmission diffraction efficiency of 32% was obtained. The efficiency was measured at a wavelength of 325 nm, and it was calculated by dividing the intensity of the first diffracted order by the intensity of the incident probe beam.

In order to investigate polymeric wavelength filters, we used a SU8 polymer (Micro Chem SU8-2005) as a core layer; this has a low optical loss (<0.4 dB/cm) and has a refractive index between 1.56 and 1.57 at a wavelength of 1.55 μm. For the fabrication of the polymeric waveguide Bragg filters, the grating was first fabricated on an OG146 polymer (n^{Te} = 1.5201 at 1.55 μm) with a length, width, and thickness of 4 cm, 1 cm, and 400 μm, respectively, by the above-mentioned process. The Bragg gratings (period: 0.5 μm; depth: 405 nm) placed on the center of the device were 0.8 mm long and 5 mm wide. A SU8 film was then spun on the polymer grating at a spin rate of 5000 rpm or 4000 rpm resulting in two different thick guiding layer (1.60 μm and 2.02 μm), and then cured at 90 °C for 5 min to form a planar waveguide (Fig. 1j). The thickness of the guiding layers was measured by using a prism coupler system (Metricon Inc., USA). After the end facet was polished, a polymeric optical filter was formed.

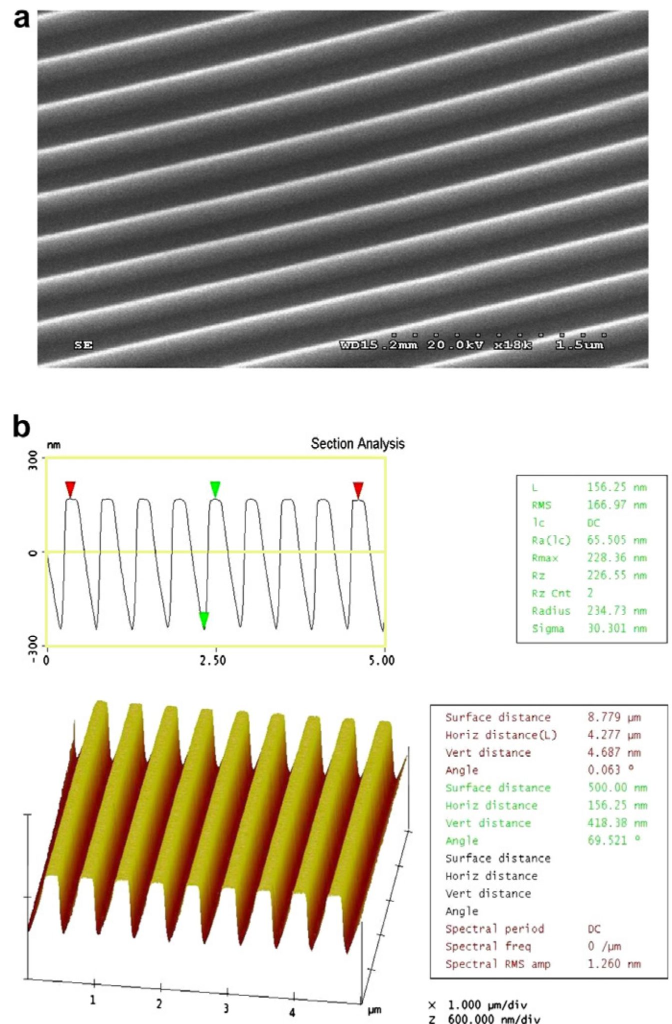

Fig. 3. The SEM and AFM micrographs of gratings on UV polymer (a) SEM, and (b) AFM (532 nm grating period and 418 nm grating depth).

In addition, a channel waveguide Bragg grating filter is fabricated in this study. A Bragg grating of the same period and depth was fabricated on the OG146 polymer using the above-mentioned process. The Bragg grating was 3-mm long and 5-mm wide. Then, a

SU-8 film was spun on the polymer grating at a spin rate of 1500 rpm. Finally, the channel waveguide pattern with a width, thickness, and length of 4.7 μm, 3.3 μm, and 4 cm, respectively, was transferred onto the grating using photolithography. Fig. 4a shows the top-view of SEM micrograph of the filter device and 4b shows the cross section of the channel waveguide.

For planar waveguide devices, the relative mode field of the polymer optical filters for a TE polarized light source at a wavelength of 1.55 μm was simulated using the beam propagation method (BPM-CAD, Opti-Wave Inc.). The effective index of the mode is 1.53968 for 1.6 μm-thick guiding layer sample and 1.547279 for 2.02 μm-thick guiding layer sample. Using the simulation, the transmission of the optical filter can be calculated by using the coupled mode theory [14,15]. The Bragg wavelength λ_B is given as $2n_{eff}\Lambda$, where n_{eff} is the mode effective index of the waveguide grating and Λ is the period of the grating. The calculated Bragg wavelength was 1539.68 nm for 1.6 μm-thick guiding layer sample and 1547.28 nm for 2.02 μm-thick guiding layer sample.

For the channel waveguide device, the effective index of the calculated effective index is 1.55043, and the calculated Bragg wavelength is 1550.43 nm.

The near field patterns of the optical waveguide were observed using the end-fire coupling technique. An amplified spontaneous emission (ASE) source with a wavelength range from 1525 to 1565 nm was used as the wide band light source (Stabilized Light Source, PTS-BBS, Newport Inc., USA). The light source was polarized in the TE direction using the in-line polarizer (ILP-55-N, Advanced Fiber Resources, China), which was followed by a polarization controller with operation wavelength around 1550 nm (F-POL-PC, Newport Inc., USA). The output mode field of the waveguide was observed using an IR CCD system (Model 7290A, Micron Viewer, Electrophysics Inc., USA) with image analysis software (LBA-710PC-D, V4.17, Spiricon Inc., USA). The measured mode field pattern of the waveguide shows the single-mode characteristics of the waveguide. Fig. 5 shows the mode field pattern of the channel waveguide device.

The spectral characteristics of the optical filter were measured using an optical spectrum analyzer. Fig. 6 shows the experimental setup of the measurement system. ASE with wavelength range from 1520 to 1565 nm was used as the wide band light source. The ASE was polarized in TE direction using the in-line fiber polarizer (NXTAR Technology Inc., Taiwan, center wavelength: 1550 nm). A He–Ne laser source as the auxiliary source was combined to the wide band source using a 2 × 1 optical fiber coupler. The optical filter was set on a micro-positioner using a waveguide holder, and two single mode fibers were used as the input and output fibers. Then the output fiber was connected to the optical spectrum analyzer to characterize the filtering performance. The measured results of the planar waveguide devices are shown in Fig. 7. In this experiment, the minimum resonant wavelength was confirmed as the Bragg wavelength. These results are similar to the theoretical predicted ones. The Bragg wavelength of the1.6 μm-thick guiding layer sample is measured at 1539 nm, and the 2.02 μm-thick guiding layer sample is measured at 1547 nm. The Bragg wavelength increased as the output fiber deviated and the deviation of the resonant wavelength is approximately 1 nm. Similarly, the Bragg wavelength of the channel waveguide filter is about 1549 nm.

For planar waveguide devices at the Bragg wavelength for the 1.6 μm-thick guiding layer sample, a transmission dip of −23 dB was obtained, and the 3-dB-transmission bandwidth was approximately 5.8 nm. For the 2.02 μm-thick guiding layer sample, a transmission dip of −16 dB was obtained, and the 3-dB-transmission bandwidth was approximately 4.5 nm. When the thickness of the guiding layer is decreased, it will result in a deep transmission

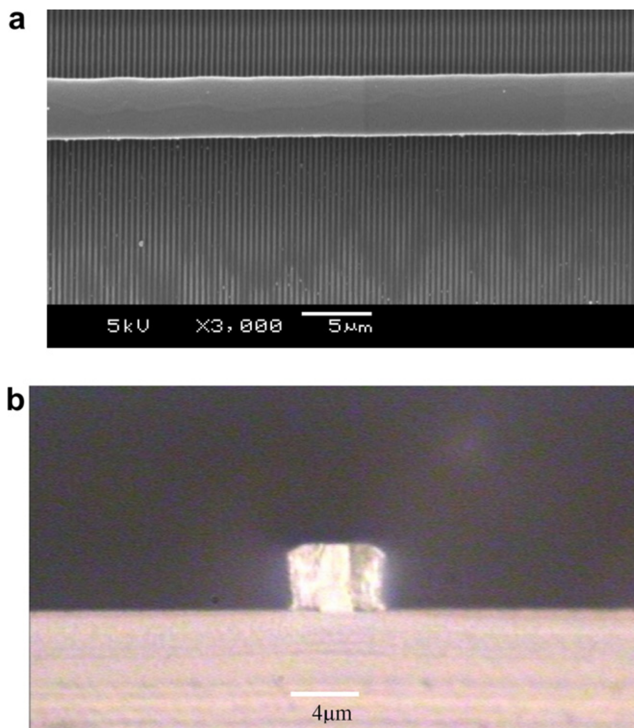

Fig. 4. (a) SEM micrograph of the channel waveguide filter, and (b) cross-section of the channel waveguide.

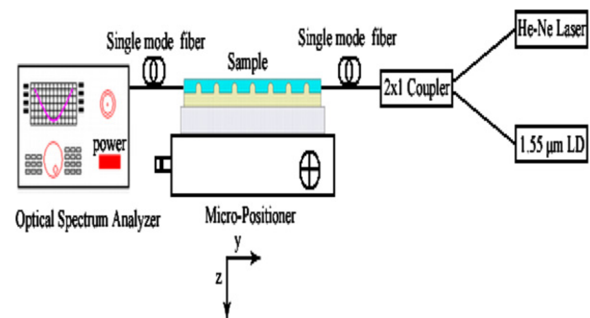

Fig. 5. Mode field pattern of the channel waveguide device.

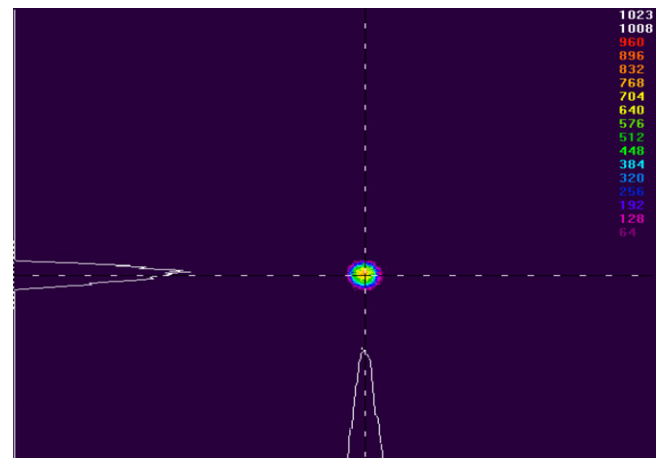

Fig. 6. Experimental setup of the transmission spectrum measurement system.

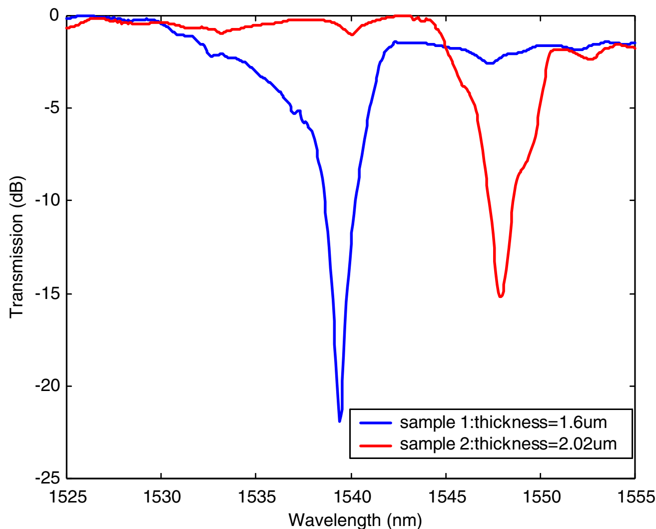

Fig. 7. Transmissio n spectrum of the polymeric wavelength filter with 0.8 mm-long grating length (sample 1: 1.6 μm thick guiding layer, sample 2: 2.02 μm thick guiding layer).

dip, thereby broadening the bandwidth. This may occur because when the thickness of the guiding layer is decreased, the mode field is broadened and then the propagation light can deeply penetrate the substrate. Therefore, the coupling coefficient between forward and backward propagation modes was increased, resulting in broadening the bandwidth and the deep transmission dip [9]. In comparison with previous results [26], the transmission bandwidth is much wider in this study due to the thinner waveguide thickness and larger grating depth, resulting in a larger coupling coefficient for our devices. The effective index of the waveguide grating was 1.53968 for 1.6 μm-thick sample and 1.547279 for 2.02 μm-thick sample, which are consistent with the experiment results.

For the channel waveguide device, the transmission spectrum is similar to the planar waveguide devices. At the Bragg wavelength, a transmission dip of approximately −13 dB was obtained and the bandwidth is approximately 4 nm.

3. Conclusion

In conclusion, we have successfully created a process to fabricate polymeric wavelength filters by using both micro-molding and holographic interference techniques. A good aspect ratio on the grating pattern could be obtained. The grating period was ~500 nm and the depth was 405 nm with 0.8-mm-long, and the grating is in the bottom of the guiding layer. For planar waveguide filter application, two different thick guiding layers were used. For the 1.6 μm thick guiding layer sample, a transmission dip of −23 dB was obtained, and the 3-dB-transmission bandwidth was about 5.8 nm. For the 2.02 μm thick guiding layer sample, a transmission dip of −16 dB was obtained, and the 3-dB-transmission bandwidth was about 4.5 nm. In addition, a channel waveguide with 4.7 μm wide, 3.3 μm high, and 4 cm in length was fabricated on the grating layer of length about 3-mm with the same period and depth as the planar waveguide filters. The transmission dip is about −13 dB and the bandwidth is approximately 4 nm at the Bragg wavelength.

References

[1] N. Imoto, J. Lightwave Technol. 3 (1985) 895.
[2] H. Hillmer, A. Grabmaier, H.L. Zhu, S. Hansmann, H. Burkhard, J. Lightwave Technol. 13 (1995) 1905.
[3] C.H. Lin, Z.H. Zhu, Y. Qian, Y.H. Lo, IEEE J. Quantum Electron. 32 (1996) 1752.
[4] Y. Shibata, S. Oku, Y. Kondo, T. Tamamura, IEEE Photon. Technol. Lett. 8 (1996) 87.
[5] A. Sharon, D. Rosenblatt, A.A. Friesem, Appl. Phys. Lett. 69 (1996) 4154.
[6] A.W. Ang, G.T. Reed, A. Vonsovici, A.G.R. Evans, P.R. Routley, M.R. Josey, IEEE Photon. Technol. Lett. 12 (2000) 59.
[7] H. Takase, A. Natansohn, P. Rochon, Polymers 44 (2003) 7345.
[8] B. Darracq, F. Chaput, K. Lahlit, Y. Levy, J.-P. Boilot, Adv. Mater. 10 (1998) 1133.
[9] A. Yarin, Introduction to Optical Electronics, third ed., H. Rinehart & Winston, New York, 1984.
[10] F. Fogli, G. Bellanca, P. Aschieri, M. Micheli, P. Bassi, J. Opt. A: Pure Appl. Opt. 6 (2004) 433.
[11] Q. Huang, P. Ashley, Appl. Opt. 36 (6) (1997) 1198.
[12] T. Ang, G. Reed, A. Vonsovici, A. Evans, P. Routley, M. Josey, IEEE Photon. Technol. Lett. 12 (1) (2000) 59.
[13] L. Zhu, Y. Huang, W. Green, A. Yariv, Opt. Express 12 (25) (2004) 6372.
[14] L. Zhu, Y. Huang, A. Yariv, IEEE Photon. Technol. Lett. 18 (6) (2006) 740.
[15] A. Kocabas, A. Aydinli, Opt. Express 14 (2006) 10228. 2006.
[16] S. Nam, J. Kang, J. Kim, Opt. Commun. 266 (2006) 332.
[17] S. Ahn, K. Lee, D. Kim, S. Lee, IEEE Photon. Technol. Lett. 17 (2005) 2122.
[18] W.C. Chuang, C.T. Ho, W.C. Wang, Opt. Express 13 (2005) 6685.
[19] D. Kim, W. Chin, S. lee, S. Ahn, K. Lee, Appl. Phys. Lett. 88 (2006) 071120-1.
[20] H. Schmid, B. Michel, Macromolecules 33 (2000) 3042.
[21] Tae-Woo Lee, Oleg Mitrofanov, Julia W.P. Hsu, Adv. Funct. Mater. 15 (2005) 1683.
[22] Kyung M. Choi, John A. Rogers, Commun. J. Am. Chem. Soc. 125 (2003) 4060.
[23] D.J. Kang, J.K. Kim, B.S. Bae, Opt. Express 12 (2004) 3947.
[24] J. Branddrup, E. Immergut, E. Grulke, Polymer Handbook, fourth ed., John Wiley and Sons, New York, 1999.
[25] J. Satnsbury, J. Ge, Photopolymerization shrinkage and stress in resins and composites, Radtech Report, May/June 2003, pp. 56.
[26] K. Kintaka, J. Nishii, T. Matano, A. Sakamoto, Jpn. J. Appl. Phys. 43 (10A) (2004) 1315.